

## Radical Polymerization Behavior of Macromonomers. 2. Comparison of Styrene Macromonomers Having a Methacryloyl End Group and a Vinylbenzyl End Group

Yasuhisa Tsukahara,<sup>\*,†</sup> Kiyoharu Tsutsumi,<sup>†</sup> Yuya Yamashita,<sup>†,‡</sup> and  
Shigetaka Shimada<sup>§</sup>

Department of Synthetic Chemistry, Faculty of Engineering, Nagoya University,  
Nagoya 464, Japan, and Department of Materials Engineering, Nagoya Institute of  
Technology, Nagoya 466, Japan

Received December 19, 1989; Revised Manuscript Received April 9, 1990

**ABSTRACT:** A study of the radical polymerization of styrene macromonomers having a methacryloyl end group (MA-PSt;  $M_n = 4400, 12\,400$ ) and a vinylbenzyl end group (VB-PSt;  $M_n = 4980, 13\,200$ ) was carried out by using gel permeation chromatography with a laser light scattering detector (LS-GPC) and electron spin resonance spectroscopy (ESR). It was shown that the degree of polymerization of poly(macromonomer)s ( $D_p$ ) measured by LS-GPC drastically varied with the macromonomer concentration in the feed ( $[M]$ ); however, there was little difference in the  $D_p$  versus  $[M]$  curves between MA-PSt and VB-PSt of the same molecular weight. The  $D_p$  of poly(macromonomer)s was small (typically less than 10) at low  $[M]$  and increased rapidly with an increase in  $[M]$  followed by the sudden decrease to  $D_p = 1$  at very high  $[M]$ . The  $D_p$  versus  $[M]$  relationship was strongly affected by the molecular weight ( $M_w$ ) of the macromonomers. These  $D_p$  versus  $[M]$  relationships were quite similar to  $D_p$  (or  $R_p$ ) versus the degree of conversion relationship of the polymerization system of conventional small monomers in the presence of the gel effect. This indicated that the diffusion-controlled effect in macromonomer systems could be clearly described by  $[M]$  and  $M_w$  of the macromonomer. It was also shown that time-conversion curves of these macromonomers were monotonic and exhibited no feature of the autoacceleration effect normally observed in the polymerization system of small monomers in the presence of the gel effect. In addition, the polymerization rate ( $R_p$ ) of MA-PSt was considerably greater than that of VB-PSt of the same molecular weight. ESR spectra of the propagating radical of MA-PSt and VB-PSt were measured to evaluate the concentration of the propagating radicals. From the results of ESR and LS-GPC, the propagation rate constant  $k_p$ , the termination rate constant  $k_t$ , and the radical lifetime  $\tau_p$  of the macromonomers are evaluated and discussed.

### Introduction

Radical polymerizations of macromonomers, i.e., macromolecular monomers, are greatly influenced by the diffusion control effect. Segmental diffusivity and translational diffusivity of the growing chains of macromonomers are strongly affected by the feed concentration and the molecular weight of the macromonomers. Furthermore, the polymerization rate of macromonomers is readily decreased upon vitrification of the polymerization system even in the presence of a polymerization solvent. Therefore, the study of the polymerization of macromonomers is of substantial interest. It provides new insights and useful information for understanding the diffusion control effect generally observed in polymerization reactions of conventional small monomers in addition to establishing fundamental knowledge for the polymerization of macromonomers. However, little attention has been paid to the polymerization of macromonomers, although there have been many attempts to prepare various kinds of macromonomers and graft copolymers of well-defined structure to develop polymeric materials of high performance and of new functions.<sup>1-17</sup> We still do not have sufficient knowledge of how the reactivity of polymerizable end groups of macromonomers is restricted by the strong diffusion control effect and how the polymer chain attached on the end group influences the polymerization reactivity of the macromonomers.

In comparison with small monomers, the molar concentration of macromonomers in a polymerization system

is usually very low even in bulk concentration; thus, the conventional dilatometric method cannot be utilized to pursue the polymerization kinetics. Furthermore, UV and NMR analyses of the characteristic peak of the polymerizable end group for the study of the polymerization kinetics are also often difficult, although these have been successfully utilized in the polymerization of small monomers for the same purpose. Previously, we have reported the radical polymerization behavior of macromonomers by using LS-GPC and ESR methods with a particular monodisperse molecular weight polystyrene macromonomer having a methacryloyl end group to show the characteristic feature of the polymerization system of macromonomers.<sup>18,19</sup> GPC equipped with LS detector in addition to RI and UV detectors is very useful in determining the true molecular weight of poly(macromonomer)s and the polymerization rate. Furthermore, ESR can provide useful information about the propagating radicals, and it has a high sensitivity in radical detection. In this paper, we have investigated the radical polymerization of styrene macromonomers having a methacryloyl end group and a vinylbenzyl end group by using the LS-GPC and ESR methods to compare the polymerization behavior of macromonomers having different types of the end group in detail. This study can provide us with new insights of how the chemical reactivity of the polymerizable end group can direct the polymerization reaction of macromonomers in the presence of the strong diffusion control effect.

### Experimental Section

**Materials.** Styrene (St) macromonomers having a methacryloyl end group (MA-PSt) were prepared by Milkovich as shown in a previous paper.<sup>18</sup> St macromonomers having a vinylbenzyl end group (VB-PSt) were prepared by the coupling

<sup>\*</sup> Nagoya University.

<sup>†</sup> Present address: Department of Industrial Chemistry, Kogakuin University, Shinjuku, Tokyo 160, Japan.

<sup>‡</sup> Nagoya Institute of Technology.

Scheme I

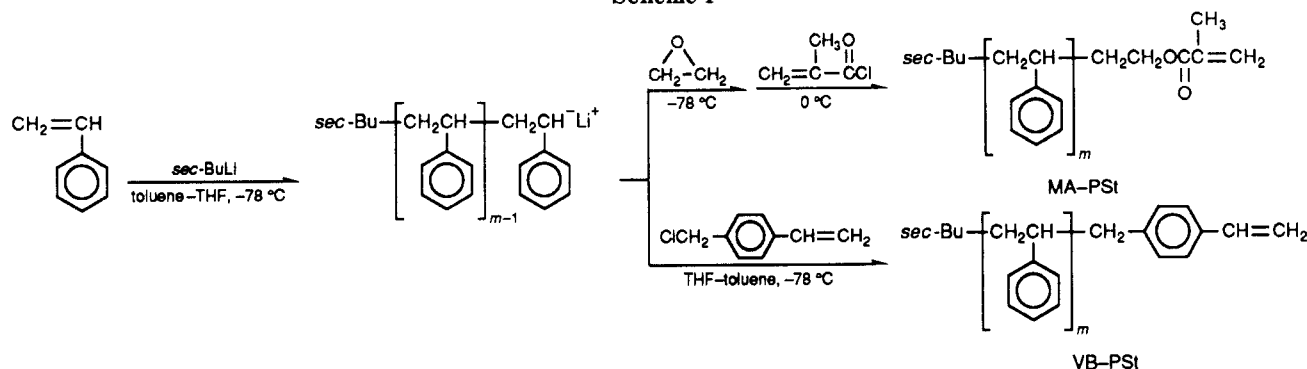


Table I  
Macromonomers of Methacryloylpolystyrene and  
(Vinylbenzyl)polystyrene

macromonomer	$M_n$	$M_w$	$M_w/M_n$	$F^a$	
				A <sup>b</sup>	B <sup>c</sup>
MA-PSt4400	4400	5400	1.23	0.88	0.82
MA-PSt12400	12400	13100	1.06	0.86	0.86
VB-PSt4980	4980	5880	1.18	0.90	0.81
VB-PSt13200	13200	13600	1.03	0.90	0.71

<sup>a</sup> End functionality. <sup>b</sup>  $F$  of MA-PSt was estimated from NMR, and that of VB-PSt was estimated from UV using the calibration curve with *p*-methylstyrene. <sup>c</sup> Maximum conversion of macromonomer in the copolymerization with MMA and AIBN in benzene at  $60^\circ\text{C}$  for 68 h. These values were used for the correction of the end functionality since  $F$  from UV is a rather rough estimation.

reaction of poly(styryllithium) living anion with an excess amount of *p*-vinylbenzyl chloride at  $-78^\circ\text{C}$  in a toluene-tetrahydrofuran (THF) mixed solvent.<sup>2,3,8</sup> Scheme I shows the preparation procedure of macromonomers. St monomer, ethylene oxide, methacryloyl chloride, azobis(isobutyronitrile) (AIBN), and solvents are commercially available. *p*-Vinylbenzyl chloride (*p*-VBC) was prepared by the chloromethylation of ( $\beta$ -bromoethyl)-benzene with chloromethyl methyl ether in the presence of  $\text{ZnCl}_2$  in dichloromethane followed by the elimination of hydrobromide with potassium *tert*-butoxide in ether according to the method employed by Asami et al.<sup>8</sup> Solvents were dried and distilled under nitrogen. AIBN was purified by recrystallization from methanol. Styrene, ethylene oxide, methacryloyl chloride, *p*-vinylbenzyl chloride, and solvents used in the living anion polymerization were dried and purified under high vacuum in the usual way. *sec*-BuLi was prepared from the reaction of *sec*-butyl chloride with Li metal in *n*-hexane. The macromonomers were precipitated into methanol and freeze-dried with benzene. The characteristics of the macromonomers used are shown in Table I.

**Polymerization of Macromonomers.** Polymerizations of macromonomers were carried out in benzene solution with AIBN as an initiator at  $60^\circ\text{C}$ . The mixture of the macromonomer, solvent, and initiator was equally divided into seven or eight parts and placed in glass ampules. Each ampule was degassed, sealed under vacuum, and placed in the thermostated bath regulated at  $60^\circ\text{C}$ , and polymerizations were then carried out for various polymerization times. After polymerization, the ampule was cooled to  $-78^\circ\text{C}$  and the polymerization product was taken out and freeze-dried with benzene.

**Evaluation of Molecular Weight and Polymerization Rate.** The molecular weights of the poly(macromonomer)s ( $M_w$ ) and the polymerization rates ( $R_p$ ) of the macromonomers were determined by using a GPC apparatus equipped with a low-angle laser light scattering detector in addition to the conventional RI and UV detectors (LS-GPC).<sup>18</sup> The radius of gyration ( $\langle S^2 \rangle_b$ ) of poly(macromonomer)s were also evaluated from LS-GPC to examine the effect of the end group on  $\langle S^2 \rangle_b$  of poly(macromonomer)s. The GPC apparatus used was a high-speed liquid chromatograph, HLC-802A of Tosoh Co. Ltd., equipped with an LS-8 (He-Ne laser with a detection angle of  $5^\circ$ ), which was operated

with Tosoh G6000H-G4000H-G2000H columns at  $25^\circ\text{C}$  on toluene (or at  $30^\circ\text{C}$  on chloroform). The solvent flow rate was 1.2 mL/min. The  $M_w$ 's of poly(macromonomer)s were determined from the peak area ratio of LS response to RI (or UV) response of polymerization products in LS-GPC. The degree of conversion was determined by the change in the peak area ratio of unreacted macromonomer to the total peak area of the polymerization product in GPC charts with consideration of end functionality.  $\langle S^2 \rangle_b$  is evaluated from the elution volume ( $V_e$ ) of poly(macromonomer)s with a  $M_w$  versus  $V_e$  calibration curve constructed with the LS detector using  $\langle S^2 \rangle = 1.38 \times 10^{-18} M_w^{1.19}$  of PSt standards in toluene at  $25^\circ\text{C}$ . The concentration of the sample injection was kept small, typically less than 0.1 wt % ( $1 \times 10^{-8}$  mol/L), to minimize the concentration effect.

**ESR Measurements.** Macromonomers and AIBN were dissolved in benzene, and the solutions were placed in an ESR sample tube (diameter 5 mm, length 180 mm) with syringes, frozen with liquid nitrogen and degassed and then sealed under vacuum. ESR spectra were taken at  $60^\circ\text{C}$  during polymerization or at  $-196^\circ\text{C}$  after quenching with liquid nitrogen. ESR measurements were carried out with a JEOL ME-3X X-band spectrometer with 100-kHz modulation. The spectra were recorded with a MELCOM 70/25 computer connected to the spectrometer.<sup>19-21</sup> The concentrations of the propagating radical  $[M^*]$  were calculated by double integration of the signal and comparison of the signal intensity with that from the standard ( $5.0 \times 10^{-6}$ – $1.0 \times 10^{-5}$  mol/L of diphenylpicrylhydrazyl (DPPH) in benzene). DPPH was purified by recrystallization from benzene before use. The signal of DPPH was used as a  $g$  value standard. The magnetic field sweep was calibrated with the splitting constant of  $\text{Mn}^{2+}$ .

## Results and Discussion

**Effect of Macromonomer Concentration on Degree of Polymerization of Poly(macromonomer)s.** Figure 1 shows plots of the weight-average molecular weights of the polymerization products, poly(macromonomer)s, of MA-PSt4400 and VB-PSt4980 ( $M_w$ ) determined with LS-GPC against macromonomer concentration in feed ( $[M]$ ) (Figure 1a), together with the degree of conversion ( $X$ ) versus  $[M]$  plots (Figure 1b). The same plots for poly(macromonomer)s from MA-PSt12400 and VB-PSt13200 are shown in parts a and b of Figure 2. In these figures, polymerizations were carried out for 24 h with initiator concentration ( $[I]$ ) =  $1.64 \times 10^{-2}$  mol/L. It is seen from Figure 1 that the  $M_w$  of poly(macromonomer)s varies uniquely as  $[M]$  increases in a manner that  $M_w$  is small and increases gradually with  $[M]$  at  $[M]$  less than ca.  $8 \times 10^{-2}$  mol/L. Then,  $M_w$  rapidly increases with  $[M]$  in the region of  $[M]$  =  $(8\text{--}14) \times 10^{-2}$  mol/L followed by a rapid decrease to  $D_p = 1$  at  $[M]$  greater than ca.  $15 \times 10^{-2}$  mol/L. This tendency is much more drastic in the cases of MA-PSt12400 and VB-PSt13200 of large molecular weight macromonomers in Figure 2a where  $M_w$  increases more rapidly in the middle concentration region of  $[M]$  =  $(4\text{--}6) \times 10^{-2}$  mol/L and then suddenly and/or discontinuously drops to  $D_p = 1$  at  $[M]$  greater than ca.  $6 \times 10^{-2}$  mol/L. The

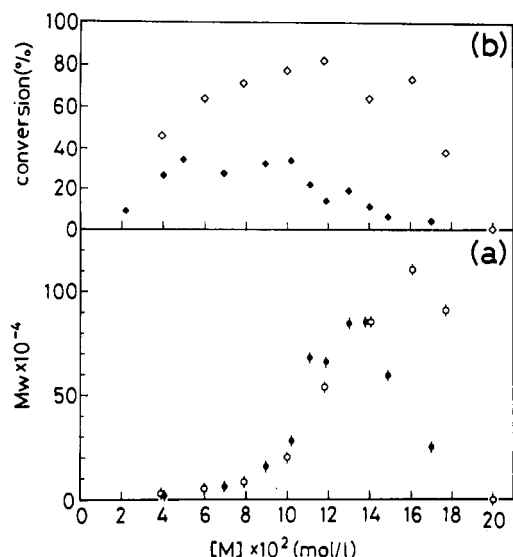


**Figure 1.** Comparison of  $M_w$  and conversion versus  $[M]$  plots of MA-PSt4400 (open symbol) and VB-PSt4980 (closed symbol): (a)  $M_w$ , (b) conversion. Polymerizations were carried out at 60 °C for 24 h with  $[I] = 1.64 \times 10^{-2} \text{ mol/L}$ .

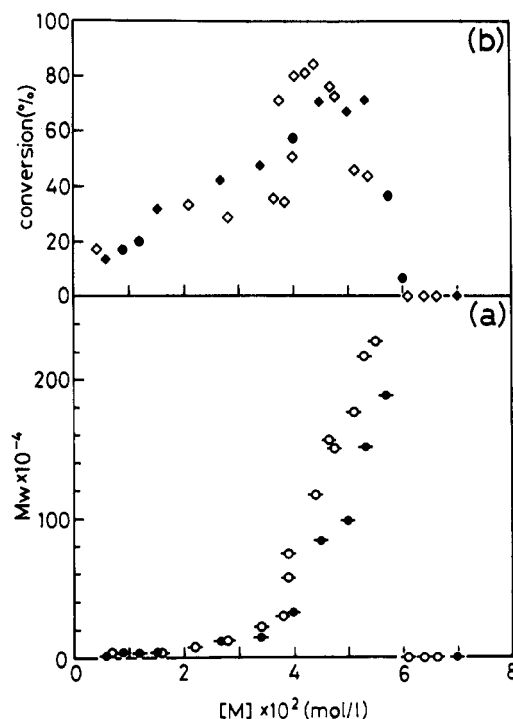


**Figure 2.** Comparison of  $M_w$  and conversion versus  $[M]$  plots of MA-PSt12400 (open symbol) and VB-PSt13200 (closed symbol): (a)  $M_w$ , (b) conversion. Polymerizations were carried out at 60 °C for 24 h with  $[I] = 1.64 \times 10^{-2} \text{ mol/L}$ .

drastic decrease of  $D_p$  at high  $[M]$  may be attributed to the vitrification phenomenon associated with the glass transition temperature of the polymerization system.

On the other hand, the degree of conversion,  $X$ , in Figure 2b varies more gradually with  $[M]$ .  $X$  values of VB-PSt4980 and MA-PSt4400 in Figure 1b do not show any characteristic dependence on  $[M]$  unlike  $M_w$ . It is of interest to note that  $X$  begins to decrease at high  $[M]$  where  $M_w$  is still continuing to increase with  $[M]$ . This may be due to a decrease of the polymerization rate at this concentration and is probably related to the decrease of the initiator efficiency ( $f$ ). It is also seen in Figure 2 that  $M_w$  of VB-PSt13200 is slightly larger than that of MA-PSt12400 at the same  $[M]$ , although the overall  $M_w$  versus  $[M]$  relationship is almost the same irrespective of the type

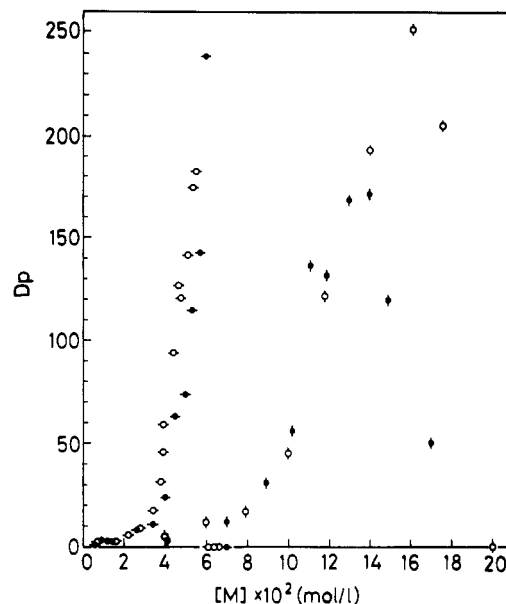


**Figure 3.** Comparison of  $D_p$  versus  $[M]$  plots of poly(macromonomer)s from macromonomers having a methacryloyl end group and a vinylbenzyl end group with different molecular weights: (○) MA-PSt4400, (◐) MA-PSt12400, (●) VB-PSt4980, (◑) VB-PSt13200.

of the polymerizable end group. In both cases,  $M_w$  can increase to over 2 million ( $D_p$  reaches 200) at around  $[M] = \text{ca. } 5.5 \times 10^{-2} \text{ mol/L}$ .

The degree of polymerization of the poly(macromonomer)s ( $D_p$ ) is plotted against  $[M]$  for all macromonomers in Figure 3 and is also summarized in Table II together with polymerization conditions and other data. It is seen from Figure 3 that the value of  $[M]$  at which  $D_p$  of the poly(macromonomer)s increases rapidly shifts to higher concentration as the molecular weight of the macromonomer decreases. This  $D_p$  (or  $M_w$ ) versus  $[M]$  relationship is very similar to the well-known  $M_w$  (or  $R_p$ ) versus degree of conversion relationship of small monomers in the presence of the autoacceleration effect or gel effect.<sup>24-26,32,33</sup> This indicates that the diffusion control effect in the macromonomer system is simply dependent on and controlled by the feed concentration and the molecular weight of the macromonomer. However, the difference in the chemical structure of the end group does not have a definite influence except that the  $D_p$  of poly(MA-PSt)s is somewhat larger than that of poly(VB-PSt)s of the corresponding molecular weight.

Since the end group of MA-PSt is methacrylate, the formation of oligo(macromonomer)s having an unsaturated end group can be also expected by the disproportionation of the propagating methacrylate radicals.<sup>22,23</sup> However, the fact that the attainable degree of polymerization of poly(macromonomer)s from VB-PSt is almost the same as that of poly(macromonomer)s from MA-PSt in Figure 3 may indicate that the effect of such oligo(macromonomer)s on the formation of large molecular weight of poly(macromonomer)s is minor and negligible, since the disproportionation reaction may be minor when the polymerizable end group is a vinylbenzyl group.

It is of interest to consider here the effect of the equilibrium monomer concentration  $[M]_e$  for the polymerization reaction in Figure 2, since the feed concentration of a macromonomer is very low.  $[M]_e$  (mol/L) values are reported as  $1.39 \times 10^{-1}$  (110 °C) and  $1.0 \times 10^{-3}$  (25 °C) for MMA, and  $1.0 \times 10^{-4}$  (110 °C) and  $1.0 \times 10^{-6}$  (25 °C) for St.<sup>29,30</sup> With these values,  $[M]_e$  for MMA at 60 °C is calculated as  $1.03 \times 10^{-2} \text{ mol/L}$  by using the Arrhenius

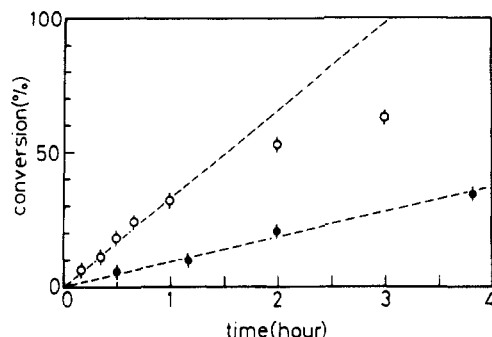


**Figure 4.** Comparison of time-conversion curves of MA-PSt4400 (open symbol,  $[M] = 11.4 \times 10^{-2}$  mol/L) and VB-PSt4980 (closed symbol,  $[M] = 11.0 \times 10^{-2}$  mol/L with  $[I] = 1.64 \times 10^{-1}$  mol/L at 60 °C.

relation. However, it is seen in Figure 2 that MA-PSt12400 having a methacryloyl end group as well as VB-PSt13200 are polymerized below  $[M] = 1 \times 10^{-2}$  mol/L although polymerization products are oligo(macromonomer)s. There is no clear sign for  $[M]_e$  around  $[M] = 1.0 \times 10^{-2}$  mol/L for MA-PSt12400. This can be ascribed to: (i) the polymerizable end group of MA-PSt is not equivalent to MMA but equivalent to methacrylate including the larger part of the ester group such as ethyl methacrylate (EMA) or 3-phenylbutyl methacrylate, and (ii) the polystyrene chain attached on the vinyl end group influences the polymerization reactivity of the end group by the steric or topological effect.

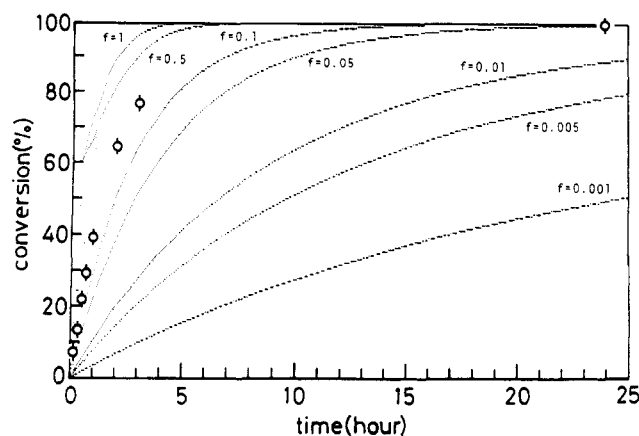
#### Time-Conversion Curves and Polymerization Rate.

Figure 4 shows the typical time-conversion curves in the cases of MA-PSt4400 and VB-PSt4980 with  $[M] = 11 \times 10^{-2}$  mol/L. The polymerization solutions were observably viscous from the initial stage at this  $[M]$ . It is seen in the figure that the polymerization rate ( $R_p$ ) of MA-PSt is clearly larger than that of VB-PSt4980 where the molecular weights of the macromonomers are nearly identical. It is also seen in Figure 4 that the degree of conversion increases (or  $R_p = dX/dt$  decreases) monotonically as the polymerization proceeds. The same feature in the time-conversion curves was also seen at different  $[M]$  and with other macromonomers of MA-PSt12400<sup>18</sup> and VB-PSt13200, indicating that this feature is very common and characteristic of the polymerization of macromonomers. However, this feature of the time-conversion curves is quite different from and in contrast to that in the polymerization of conventional small monomers in the presence of the gel effect where a remarkable autoacceleration of the polymerization rate is normally observed as polymerization proceeds under isothermal condition. Absence of acceleration of polymerization rate with polymerization time was also seen in the  $M_w$  versus  $X$  (or polymerization time) relationship in our previous paper.<sup>18</sup> This feature is reasonably explained on the basis that the gel effect appears from the beginning of the polymerization reaction in the macromonomer system because of the high viscosity of the polymerization media due to the presence of macromolecular monomers. Therefore,  $M_w$  of poly(macromonomer)s changes greatly as  $[M]$  increases. On the other hand,  $M_w$  did not depend much upon the degree of conversion because the degree of gel effect does not change much as polymerization proceeds.

In the radical polymerization, it is well-known that  $R_p$  is given by the relation

$$R_p = k_p[M]_t \left( \frac{fk_d[I]_t}{k_t} \right)^{1/2} \quad (1)$$

where  $[I]_t$  and  $[M]_t$  are the initiator and macromonomer



**Figure 5.** Replots of time-conversion data of MA-PSt4400 in Figure 4 including high conversion data on the calculated curves using eq 2 with various initiator efficiency,  $f$ . Kinetic parameters used were  $k_d = 1.01 \times 10^{-5}$  s<sup>-1</sup>,  $k_p = 22$  L/mol·s, and  $k_t = 8400$  L/mol·s. Experimental data were corrected with the end functionality of MA-PSt4400 (0.82).

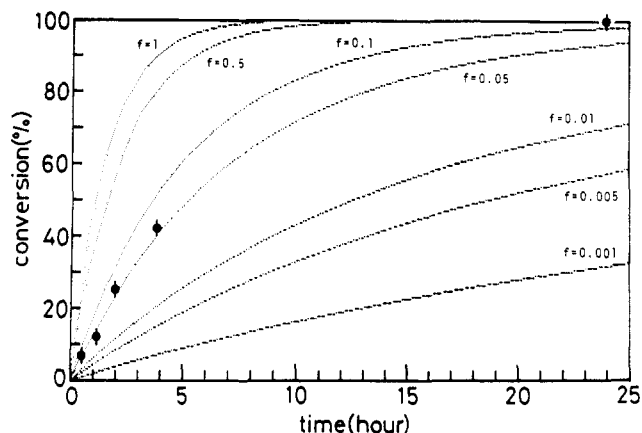


**Figure 6.** Replots of time-conversion data of VB-PSt4980 in Figure 4 including high conversion data on the calculated curves using eq 2 with various initiator efficiency,  $f$ . Kinetic parameters used were  $k_d = 1.01 \times 10^{-5}$  s<sup>-1</sup>,  $k_p = 5$  L/mol·s, and  $k_t = 1300$  L/mol·s. Experimental data were corrected with the end functionality of VB-PSt4980 (0.81).

concentrations at the degree of conversion  $X$  at polymerization time  $t$ .  $k_p$ ,  $k_t$ ,  $k_d$ , and  $f$  are the propagating rate constant, termination rate constant, decomposition rate constant, and initiator efficiency, respectively.  $[I]_t$  is also given by  $[I]_t = [I] \exp(-k_d t)$ . Rearrangement and integration of eq 1 from  $X = 0$  to  $X = X$  leads to

$$-\ln([M]_t/[M]) = -\ln(1 - X) = 2k_p \left( \frac{2f[I]_t}{k_t k_d} \right)^{1/2} (1 - e^{-k_d t/2}) \quad (2)$$

This is a well-known expression for dead-end polymerization.<sup>27-29</sup> In Figures 5 and 6, time-conversion curves in the case of MA-PSt4400 and VB-PSt4980 with termination by radical coupling calculated from eq 2 are shown by using  $k_p = 22$  L/mol·s and  $k_t = 8400$  L/mol·s for MA-PSt4400 and  $k_p = 4.8$  L/mol·s and  $k_t = 1300$  L/mol·s for VB-PSt4980, and  $k_d = 1.01 \times 10^{-5}$  s<sup>-1</sup>,  $[M] = 1.1 \times 10^{-1}$  mol/L, and  $[I] = 1.64 \times 10^{-1}$  mol/L. The details of these parameters are discussed in the following section. The experimental time-conversion data are plotted on the calculated curves in Figures 5 and 6 after correction of the end functionality (0.82 for MA-PSt4400 and 0.81 for VB-PSt4980). It is seen in the figure that the experimental time-conversion curves are consistent with the calculated curves. If the gel effect does not influence the time-conversion curve or does not change as the polymerization

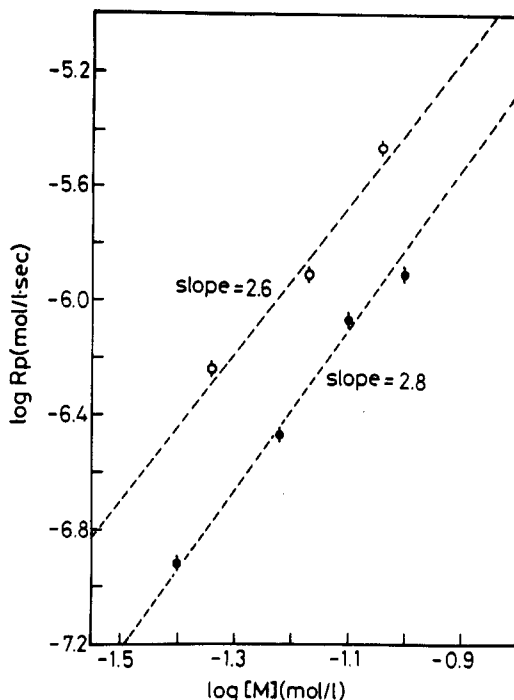


**Figure 7.** log-log plots of  $R_p$  versus  $[M]$  of MA-PSt4400 (open symbol) and VB-PSt4980 (closed symbol). Polymerizations were carried out with  $[I] = 1.64 \times 10^{-2}$  mol/L in benzene at 60 °C.

proceeds, Figures 5 and 6 yield the initiator efficiency of each polymerization by fitting eq 2 to the experimental time-conversion data.  $f$  estimated from Figures 5 and 6 is ca. 0.2 for MA-PSt4400 and ca. 0.05 for VB-PSt4980. The corresponding  $f$  value for termination by disproportionation estimated in this way was 0.1 for MA-PSt4400 and 0.03 for VB-PSt. The termination by disproportionation is more likely to occur in macromonomer polymerization systems, especially for MA-PSt4400. Figures 5 and 6 indicate that the gel effect also is almost constant as polymerization proceeds. The initiator efficiency also can be directly evaluated from the decay curve of the DPPH radical in the ESR spectrum. The  $f$  value for MA-PSt4400 obtained by ESR with  $[M] = 11.4 \times 10^{-2}$  mol/L,  $[I] = 1.64 \times 10^{-1}$  mol/L, and  $[DPPH] = 3.28 \times 10^{-3}$  mol/L at 60 °C was 0.05–0.1 and almost the same order to  $f$  obtained in Figure 5. Russell, Napper, and Gilbert recently reported on the initiator efficiency variation in the radical polymerization of MMA where  $f$  decreases gradually to 0.1 at first as the weight fraction of polymer  $w_p$  increases and then markedly decreases at  $w_p$  greater than 0.84 due to the increase of viscosity in the polymerization system.<sup>31</sup> The value of  $f$  obtained in Figures 5 and 6 indicates that the polymerizations in Figures 5 and 6 belong to the region near or beyond the critical  $w_p$  (0.84) where the cage effect is marked.

In Figures 7 and 8,  $R_p$  values of MA-PSt and VB-PSt determined from the initial slope of time-conversion curves are plotted against  $[M]$ . In these figures,  $[M]$  is corrected with the end functionality,  $F$ . It is seen from the figure that  $R_p$  values of MA-PSt4400 and MA-PSt12400 are substantially larger than those of VB-PSt4980 and VB-PSt13200, respectively. This means that the polymerizable end group bearing a long PSt chain can still influence  $R_p$ . The larger value of  $R_p$  of the MMA monomer than that of the St monomer is preserved in the presence of a strong diffusion control effect. In addition,  $R_p$  values of MA-PSt12400 and VB-PSt13200 are larger than those of MA-PSt4400 and VB-PSt4980 at the same  $[M]$ . This is because the gel effect becomes larger as the molecular

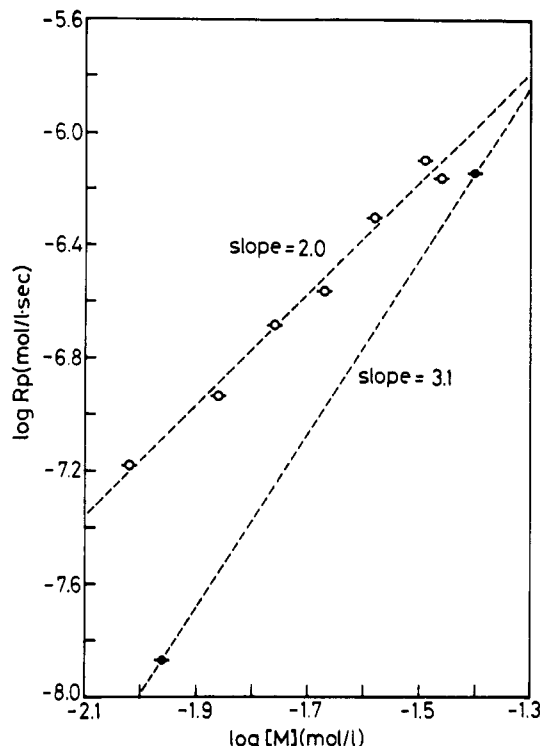


**Figure 8.** log-log plots of  $R_p$  versus  $[M]$  of MA-PSt12400 (open symbol) and VB-PSt13200 (closed symbol). Polymerizations were carried out with  $[I] = 1.64 \times 10^{-2}$  mol/L in benzene at 60 °C.

weight increases at the same macromonomer concentration. The slopes of the straight lines fitted to the data on the log  $R_p$  versus log  $[M]$  graph are 2.6 for MA-PSt4400 and 2.8 for VB-PSt4980 in Figure 7 and 2.0 for MA-PSt12400 and 3.1 for VB-PSt13200 in Figure 8 with  $[I] = 1.64 \times 10^{-2}$  mol/L. Obviously, these high orders of  $R_p$  with respect to  $[M]$  can be attributed to the  $[M]$ -dependent gel effect.

**Results of ESR Measurements.** In this section, we discuss the results of ESR spectroscopy applied to the radical polymerization of these macromonomers. By using ESR, one can obtain direct information on the propagating radical, such as the concentration, lifetime, and chemical structure of the radical species. In Figure 9, ESR spectra of MA-PSt4400 and VB-PSt4980 are shown; these were measured at -196 °C after quenching from 60 °C with liquid N<sub>2</sub>. Quenching was performed after 30 min of polymerization. The ESR spectrum of MA-PSt4400 is almost the same as those of the MMA propagating radicals in the literature and that of MA-PSt12400 previously reported.<sup>19</sup> It is characterized by nine lines consisting of five strong lines having a hyperfine splitting constant of 23.4 G and four weak lines, appearing between the five lines. On the other hand, the ESR spectrum of VB-PSt4980 is quite different from that of MA-PSt but resembles that of the propagating radical of St monomer in an emulsion system,<sup>34</sup> where the spectrum is considerably broadened and the hyperfine structure of the propagating radical is not clear<sup>38</sup> due to the viscosity of the polymerization media. It is seen from the figure that the growing radical of the macromonomer having a vinylbenzyl end group is also stable and detectable by ESR spectroscopy.

From the ESR spectra, the concentration of the propagating radical of macromonomers,  $[M^*]$ , was directly evaluated from the signal intensity by comparison of the signal with that from the standard containing a known concentration of DPPH.  $[M^*]$  values of MA-PSt4400 and VB-PSt4980 evaluated from the ESR spectra measured

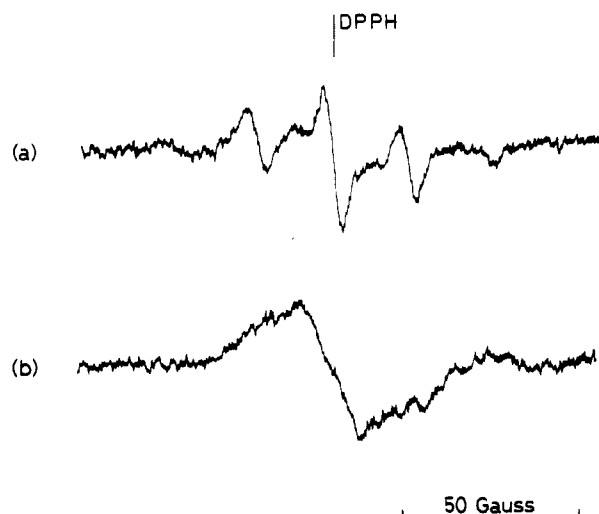


**Figure 9.** ESR spectra of the propagating radicals of macromonomers taken after quenching from +60 to -196 °C. Polymerizations were carried out for 30 min with  $[I] = 1.64 \times 10^{-2}$  mol/L: (a) MA-PSt4400,  $[M] = 11.4 \times 10^{-2}$  mol/L, (b) VB-PSt4980,  $[M] = 11.0 \times 10^{-2}$  mol/L. Sweep time is 4 min/200 G, response time is 0.3 s. The vertical line in the figure is DPPH;  $g = 2.0036$ .

at 30 min of polymerization time at -196 °C are shown in Table III.  $[M^*]$  values in Table III are the average values obtained from five independent measurements under the same polymerization conditions. It can be seen from the table the concentrations of the propagating radicals of macromonomers in this work are of the order of  $10^{-6}$  mol/L and considerably higher than those of conventional small monomers in solution polymerization of the same range of  $[M]$ .

By combination of  $[M^*]$  in Table III with  $D_p$  and  $R_p$  determined from LS-GPC, the propagating rate constant,  $k_p$ , the termination rate constant,  $k_t$ , and the radical lifetime,  $\tau_p$ , were evaluated by using the relations<sup>35-37</sup>

$$-d[M]/dt = k_p[M^*][M] \quad (3)$$

$$k_t = (-d[M]/dt)(1/2\nu_p[M^*]^2) \quad (4)$$

$$\tau_p = \nu_p/k_p[M] \quad (5)$$

where  $\nu_p$  is the kinetic chain length. The kinetic parameters calculated from eqs 3-5 for MA-PSt4400 and VB-PSt4980 are also shown in Table III as a preliminary result. In these equations, the bimolecular termination of the propagating radicals is assumed to derive eq 4, while no assumption is made in eqs 3 and 5. Furthermore, in eq 4,  $D_p = 2\nu_p$  for the bimolecular termination by coupling, and  $D_p = \nu_p$  for the termination by disproportionation. Both  $k_t$ 's for  $D_p = 2\nu_p$  and  $D_p = \nu_p$  are shown in Table II.

$k_p$  and  $k_t$  values (L/mol·s) of the corresponding small monomers (MMA and St) are reported as  $k_p(\text{MMA}) = 515$  and  $k_t(\text{MMA}) = 2.6 \times 10^7$  and  $k_p(\text{St}) = 165$  and  $k_t(\text{St}) = 6.0 \times 10^7$  at 60 °C.<sup>29,30</sup> It is seen from Table III that  $k_p$  as well as  $k_t$  of macromonomers are much smaller than those of the corresponding small monomers due to the diffusion control effect.  $k_p$  and  $k_t$  of VB-PSt4980 are about 1/40 and 1/90000 and  $k_p$  and  $k_t$  of MA-PSt4400 are about 1/20 and 1/3000 of those of small monomers.  $k_t$  for the radical polymerization of a different type of macromonomer in benzene was reported very recently by Hatada, Kitayama, and Kamachi by the ESR method. Their  $k_t$  for a *syn*-PMMA macromonomer having a vinylbenzyl end group obtained from the signal decay is 600 L/mol·s under

**Table II**  
Characterization of Poly(macromonomer)s of MA-PSt4400, MA-PSt12400, VB-PSt4980, and VB-PSt13200<sup>a</sup>

run	$[M] \times 10^2$ , mol/L	$M_w \times 10^{-4}$ LS	$ec^b$	$D_p$	conv, %	$\langle S^2 \rangle_b^{1/2}$ , nm	$\langle S^2 \rangle_t^{1/2,c}$ , nm	$g$
MA-PSt4400								
1	1.99	3.0	1.8	6.8	8.4	3.98	5.4	0.539
2	3.99	3.7	2.4	8.4	32.2	4.77	6.12	0.607
3	5.50	7.5	3.4	17.1	57.5	5.81	9.35	0.386
4	6.00	6.7	2.0	15.3	64.0	4.93	8.8	0.317
5	6.89	6.8	3.8	15.5	51.7	6.21	8.84	0.493
6	7.91	17.9	4.0	40.7	71.3	6.21	15.7	0.156
7	10.0	26.2	6.2	590.5	77.8	7.77	19.7	0.156
8	10.4	18.5	6.5	42.0	75.5	8.54	16.0	0.285
9	10.9	44.7	11.0	102	80.0	11.7	27.0	0.188
10	11.6	50.1	12.6	114	81.8	12.7	28.9	0.193
11	11.8	57.5	10.4	131	80.0	9.36	31.4	0.0889
12	12.6	67.2	14.3	153	80.4	13.7	34.5	0.158
13	14.0	99.7	18.1	227	64.3	14.3	43.6	0.108
14	16.1	93.7	21.4	213	73.6	15.6	42.0	0.138
15	17.7	128	25.1	291	38.0	17.3	50.6	0.117
MA-PSt12400 <sup>d</sup>								
1	2.53	47.6	13.1	36.3	30.7	13.8	28.1	0.241
2	3.76	27.4	10.8	20.9	68.7	11.5	20.2	0.324
3	4.22	165	25.4	126	74.4	16.1	58.8	0.0750
4	4.68	154	43.3	118	69.9	17.5	56.4	0.0963
5	5.12	175	43.1	134	45.9	18.8	60.9	0.0953
6	5.37	195	52.3	149	42.4	17.3	64.9	0.0710
7	5.50	220	40.0	168	52.4	18.8	69.8	0.0725
VB-PSt4980								
1	6.95	22.4	3.33	45.0	27.4	5.45	17.9	0.0927
2	8.92	21.8	5.43	43.8	32.4	7.11	17.6	0.163
3	11.1	47.8	12.9	96.0	21.9	11.3	28.1	0.161
4	11.9	49.8	14.2	100	13.8	11.3	28.8	0.153
5	13.0	64.5	16.1	130	19.2	14.2	33.6	0.178
6	14.0	70.1	14.1	141	11.3	13.4	35.3	0.144
7	14.9	56.7	13.5	114	6.0	11.2	31.1	0.129
VB-PSt13200								
1	2.66	16.7	6.99	12.7	42.1	8.88	15.0	0.350
2	3.40	41.6	8.78	31.5	47.0	10.0	25.9	0.149
3	3.98	48.9	13.8	37.0	57.0	12.5	28.5	0.192
4	4.49	187	15.0	142	70.4	14.7	63.3	0.0539
5	5.00	208	22.7	158	67.2	15.2	67.5	0.0507
6	5.33	224	25.7	170	71.1	16.3	70.5	0.0534
7	5.71	260	30.3	197	36.3	16.3	77.1	0.0447

<sup>a</sup> Polymerizations were carried out in benzene at 60 °C for 24 h with  $[I] = 1.64 \times 10^{-2}$  mol/L.  $[M]$  values are as feed values (without correction by  $F$ ). <sup>b</sup> Apparent molecular weight calculated with the calibration curve of the PSt standards. <sup>c</sup>  $\langle S^2 \rangle^{1/2}$  of linear PSt of corresponding  $M_w$  estimated from  $\langle S^2 \rangle = 1.38 \times 10^{-18} M_w^{1.19}$ . <sup>d</sup> See also Tables I and III of ref 18.

irradiation of UV light in the presence of AIBN. This value is almost the same order as that of our VB-PSt4980.

In the polymerization of small monomers in the absence of the diffusion control effect,  $k_p(\text{MMA})$  is larger than  $k_p(\text{St})$  and  $k_t(\text{St})$  is larger than  $k_t(\text{MMA})$  due to the resonance effect in the reactivity of the St monomer and the stability of the styryl radical. The radical lifetime,  $\tau_p$ , of VB-PSt4980 is also larger than that of MA-PSt4400. Therefore, the result in Table III suggests that the end group still directs the polymerization reaction under such a strong diffusion control effect as shown in the previous section.

In the evaluation of  $k_p$ ,  $k_t$ , and  $\tau_p$  with eqs 3-5, the contribution of the primary radical termination<sup>39</sup> and the unimolecular termination<sup>28,29</sup> should also be taken into account. The primary radical termination is likely to occur in the macromonomer system because of the low concentration of the macromonomers and the specific multi-branched structure of the propagating radicals as described previously.<sup>18</sup> Moreover, as  $[M]$  or  $M_w$  of the macromonomer increases, the viscosity of the polymerization system increases rapidly. This significantly decreases both the

Table III  
Propagating Rate Constant  $k_p$ , Termination Rate Constant  $k_t$ , and Radical Lifetime of the Propagating Chain  $\tau_p$

macromonomer	feed concn, $\times 10^2$ mol/L		$D_p$	$R_p \times 10^6$ , mol/L·s	$[M^*] \times 10^6$ , <sup>a</sup> mol/L	$k_p$ , <sup>b</sup> L/mol·s	$k_t$ , <sup>b</sup> L/mol·s		$\tau_p$ , <sup>b</sup> s
	[M]	[I]					coupling	dispro	
VB-PSt4980	11.0 (8.9) <sup>c</sup>	16.4	59	2.81	$7 \pm 1$	$4 \pm 1$ (5)	$1300 \pm 450$	$630 \pm 230$	$160 \pm 23$
MA-PSt4400	11.4 (9.3)	16.4	54	10.4	$6 \pm 2$	$18 \pm 5$ (22)	$8400 \pm 3800$	$4200 \pm 1100$	$33 \pm 8$

<sup>a</sup>  $[M^*]$  was evaluated from the ESR signal intensity ratio of the propagating radicals to that of DPPH standard of known concentration.

<sup>b</sup> Deviations were calculated from  $z_{av} \pm 0.6745 [\Sigma(z_i - z_{av})^2 / (n - 1)]^{1/2}$ . <sup>c</sup> Value in the parentheses is that corrected by the end functionality,  $F$ .

initiator efficiency and the segmental diffusivity. Thus, at very high  $[M]$ , the primary radical termination begins to be suppressed and alternatively the propagating radical can be occluded as a stable macroradical by the unimolecular termination.

Since the unimolecular termination does not contribute to the rate of disappearance of the propagating radical, the termination rate  $R_t$  is expressed by

$$R_t = 2k_t[M^*]^2 + k_{t,prim}[R^*][M^*] \quad (6)$$

where  $k_{t,prim}$  is the rate constant for the primary radical termination and  $[R^*]$  is concentration of the primary radical. In this case, the termination rate constant for the bimolecular termination,  $k_t$ , is given by eq 7 instead of eq

$$k_t = \left( \frac{k_p[M]}{2\nu_p[M^*]} \right) - \left( \frac{k_{t,prim}[R^*]}{2[M^*]} \right) \quad (7)$$

4, while,  $\tau_p$  can be given by eq 4 even when primary radical termination is involved. Therefore,  $k_t$  in Table III can be considered to involve the contribution of the primary termination reaction.  $k_t$  from eq 7 is smaller than the value in Table III depending on  $k_{t,prim}$  and the ratio  $[R^*]/[M^*]$ . It is difficult, however, to evaluate  $k_t$  and  $k_{t,prim}$  separately from the data in Table III at present. Further studies having the purpose of understanding the molecular weight dependence of  $k_p$ ,  $k_t$ , and  $\tau_p$  and the contribution of the primary radical termination and the unimolecular termination are now in progress and will appear elsewhere.

**Effect of Backbone on the Chain Dimension of Poly(macromonomer)s.** Finally, we briefly discuss the effect of the polymerizable end group on the molecular dimensions and the determination of the molecular weight of produced poly(macromonomer)s. The backbone of poly(macromonomer)s from MA-PSt is composed of methacrylate segments, and thus the resulting poly(MA-PSt)s are not pure PSt. The nature of the backbone segment can affect the GPC determination of the molecular weights of poly(macromonomer)s as well as the polymerization kinetics, especially when the fraction of the end group is relatively large, i.e., when the molecular weight of the macromonomer becomes small. Therefore, it is worthwhile to compare the molecular dimension of poly(macromonomer)s of MA-PSt with that of VB-PSt.

In Figure 10,  $g$  values, the ratios of the mean-square radius of gyration of poly(macromonomer)s to that of linear polymer of the same molecular weight ( $\langle S^2 \rangle_b / \langle S^2 \rangle_l$ ) are plotted against  $D_p$ .  $\langle S^2 \rangle_b$  was estimated from the elution volume,  $V_r$ , in GPC by using  $\langle S^2 \rangle$  versus  $V_r$  calibration curve, which was constructed by combining the empirical  $M_w$  versus  $V_r$  curve of the standard linear PSt samples on toluene at 25 °C with  $\langle S^2 \rangle_l = 1.38 \times 10^{-18} M_w^{1.19}$  assuming  $V_r$  of linear and branched polymer molecules correlation with their molecular dimension  $\langle S^2 \rangle$  in a same manner.<sup>18</sup> It can be seen from Figure 10 that  $g$  values decrease rapidly and monotonically as  $D_p$  increases due to the increased compactness of the poly(macromonomer)s. These  $g$  versus  $D_p$  relationships are almost the same for both poly(MA-

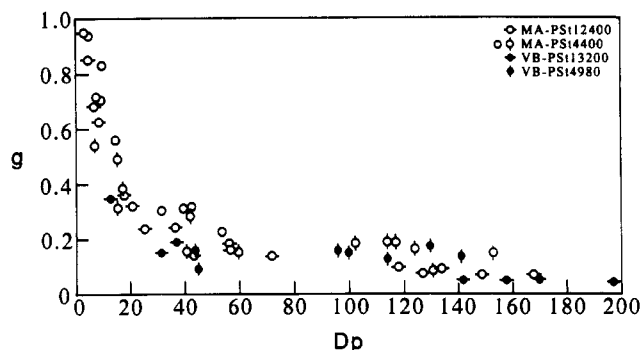


Figure 10. Comparison of  $g$  versus  $D_p$  plots of poly(MA-PSt)s (open circle) and poly(VB-PSt)s (closed circle) measured in toluene at 25 °C: (○) poly(MA-PSt4400), (□) poly(MA-PSt12400), (●) poly(VB-PSt4980), (◐) poly(VB-PSt13200). These were prepared with  $[I] = 1.64 \times 10^{-2}$  mol/L. (○) Data for poly(MA-PSt4400) with  $[I] = 16.4 \times 10^{-2}$  mol/L.

PSt) and poly(VB-PSt), except that the  $g$  values of poly(VB-PSt)s are slightly smaller than those of poly(MA-PSt)s at the same  $D_p$ . The slight difference in  $g$  may possibly be ascribed to the stiffer nature of the methacrylate backbone segment of poly(MA-PSt)s. However, Figure 10 indicates that the difference is small and can be neglected in these molecular weights of macromonomers. Furthermore, it can be seen that the  $g$  values of poly(MA-PSt4400) and poly(VB-PSt4980) are slightly larger than those of poly(MA-PSt12400) and poly(VB-PSt13200), respectively, due to the increased contribution of the backbone segments.

## References and Notes

- Yamashita, Y.; Tsukahara, Y. In *Modification of Polymers*; Carraher, C., Moore, J., Eds.; Plenum Press: New York, 1983; p 131.
- Tsukahara, Y.; Kohno, K.; Inoue, H.; Yamashita, Y. *Nippon Kagaku Kaishi* 1985, 1070.
- Tsukahara, Y.; Tsai, C.-H.; Yamashita, Y.; Muroga, Y. *Polym. J.* 1987, 19, 1033.
- Nishimura, T.; Maeda, M.; Nitadori, Y.; Tsuruta, T. *Makromol. Chem., Rapid. Commun.* 1980, 1, 573.
- Tezuka, Y.; Okabayashi, A.; Imai, K. *Makromol. Chem.* 1989, 190, 753.
- Ito, K.; Usami, N.; Yamashita, Y. *Macromolecules* 1980, 13, 216.
- Kawakami, Y.; Miki, Y.; Tsuda, T.; Murthy, R. A. N.; Yamashita, Y. *Polym. J.* 1982, 14, 913.
- Asami, R.; Takaki, M.; Hatanaka, H. *Macromolecules* 1983, 16, 628.
- Rempp, P. F.; Franta, E. *Adv. Polym. Sci.* 1984, 58, 1.
- Schulz, G. O.; Milkovich, R. *J. Polym. Sci., Polym. Chem. Ed.* 1984, 22, 1633.
- Fukutomi, T.; Yokota, A.; Ishizu, K. *J. Polym. Sci., Polym. Chem. Ed.* 1984, 22, 2983.
- Hatada, K.; Shinozaki, T.; Ute, K.; Kitayama, T. *Polym. Bull.* 1988, 19, 231.
- Hashimoto, K.; Sumitomo, H.; Kawasumi, M. *Polym. J.* 1985, 17, 1045.
- Kobayashi, S.; Saegusa, T. *Polym. Bull.* 1983, 9, 169. Miyamoto, M.; Maki, K.; Tokumizu, M.; Saegusa, T. *Macromolecules* 1989, 22, 1604.
- Sawamoto, M.; Enoki, T.; Higashimura, T. *Polym. Bull.* 1986, 16, 117.
- Farona, M. F.; Kennedy, J. P. *Polym. Bull.* 1984, 11, 359.

- (17) Muhlbach, K.; Percec, V. *J. Polym. Sci., Polym. Chem. Ed.* **1987**, *25*, 2605.
- (18) Tsukahara, Y.; Mizuno, K.; Segawa, A.; Yamashita, Y. *Macromolecules* **1989**, *22*, 1546.
- (19) Tsukahara, Y.; Tsutsumi, K.; Yamashita, Y.; Shimada, S. *Macromolecules* **1989**, *22*, 2869.
- (20) Kashiwabara, H.; Shimada, S.; Hori, Y.; Sakaguchi, M. *Adv. Polym. Sci.* **1987**, *82*, 141.
- (21) Shimada, S.; Hori, Y.; Kashiwabara, H. *Macromolecules* **1988**, *21*, 2107.
- (22) Cacioli, P.; Hawthorne, D. G.; Laslett, R. L.; Rizzardo, E.; Solomon, D. H. *J. Macromol. Sci., Chem.* **1986**, *A23*, 839.
- (23) Tanaka, H.; Kawai, H.; Sato, T.; Ota, T. *J. Polym. Sci., Polym. Chem. Ed.* **1989**, *27*, 1741.
- (24) Tulig, T.; Tirrell, M. *Macromolecules* **1981**, *14*, 1501.
- (25) Mita, I.; Horie, K. *J. Macromol. Sci., Rev.* **1987**, *C27*, 91.
- (26) Nishimura, N. *J. Macromol. Chem.* **1964**, *1*, 257.
- (27) Tobolsky, A. V. *J. Am. Chem. Soc.* **1958**, *80*, 5927.
- (28) Otsu, T. *Radical Polymerization. I*, Japanese; Kagaku Dojin: Kyoto, 1971.
- (29) Odian, G. *Principles of Polymerization*, 2nd ed.; Wiley: New York, 1981.
- (30) Brandrup, J.; Immergut, E. H., Eds. *Polymer Handbook*, 2nd ed.; Wiley: New York, 1975.
- (31) Russell, G. T.; Napper, D. H.; Gilbert, R. G. *Macromolecules* **1988**, *21*, 2141.
- (32) Zhu, S.; Hamielec, A. E. *Macromolecules* **1989**, *22*, 3093.
- (33) Yokota, K. *Koubunsi* **1970**, *19*, 566.
- (34) Ballard, M. J.; Gilbert, R. G.; Napper, D. H.; Pomery, P. J.; O'Donnell, J. H. *Macromolecules* **1984**, *17*, 504.
- (35) Rånby, B.; Rabek, J. F. *ESR Spectroscopy in Polymer Research*; Springer-Verlag: Berlin, 1977.
- (36) Kamachi, M. *Adv. Polym. Sci.* **1987**, *82*, 207.
- (37) Bresler, S. E.; Kazbekov, E. N.; Shadrin, V. N. *Makromol. Chem.* **1974**, *175*, 2875.
- (38) Bresler, S. E.; Kazbekov, E. N.; Fomichev, V. N.; Shadrin, V. N. *Makromol. Chem.* **1972**, *157*, 167.
- (39) Bamford, C. H.; Jenkins, A. D.; Johnston, R. *Trans. Faraday Soc.* **1959**, *55*, 1451.
- (40) Hatada, K.; Kitayama, T.; Masuda, E.; Kamachi, M. *Polym. Prepr. Jpn.* **1989**, *38*, 1314; *Makromol. Chem., Rapid Commun.* **1990**, *11*, 101.